

Enhanced Effective Detection of Buried Radioactive Waste - 10177

Qian Du ¹, Wei Wei ¹, Zhongyuan Huang ¹, Nicolas H. Younan ¹, Charles Waggoner ²,
Donna Rogers ²

¹ Department of Electrical and Computer Engineering
² Institute for Clean Energy Technology
Mississippi State University, MS 39762, USA

ABSTRACT

In our previous paper, we presented a matched filtering (MF)-based approach to detect buried radioactive waste using its gamma-ray spectrum. This approach does not require background information and its performance is robust under very low-count conditions. In this paper, we improve this approach when background information is available. The spectral comparison ratio (SCR) method is adopted to normalize the background contribution in energy spectra, and the MF operator is applied on the SCR-transformed data. The resulting SCR MF approach can improve the performance of MF. It can also outperform other widely used techniques, such as energy window and gross count.

INTRODUCTION

The detection of radioactive materials has many critical applications. For instance, the detection of the transportation of illicit nuclear materials from manufacturing and storage facilities and the radioactive sources in steel scrap entering reprocessing facilities become more and more important at international borders [5,6,7]. As a result, the radial portal monitor devices, consisting of gamma-ray detectors and often neutron detectors, are major devices used in the detection. Many discussions on plastic and sodium iodide (NaI) scintillation detectors for detecting special nuclear materials (SNM) show that plastic detectors are low-cost and light which enables large detectors to be employed while NaI detectors have higher sensitivity because of their enhanced resolution [8].

Various methods have been proposed for the detection of SNM at border screening [9,10,11]. Some of them developed the Gross Count (GC) method which is widely used. It focuses on counting all the gamma photons distributing over all the energy bands. It can differentiate naturally occurring radioactive material (NORM) from the background [9], but may not be able to discriminate different NORMs. Another method of energy window (EW) is to compare the shape of energy distribution in several windows with background which is much improved than a simple GC method [9]. According to the shape of energy peak, referred to as the feature, template identification technique may improve the detection performance as well [11].

When radioactive waste or SNM is buried, energy counts can be very low. The performance of the aforementioned methods may be limited. In our previous research, we employed matched filtering (MF) to achieve its detection [1]. First, important features are extracted from the gamma

spectroscopy collected when a penetrator is located on the surface; then, an MF-based detector is applied to the spectrum when the penetrator is buried using the extracted features. Even when the background information is unavailable, the algorithm still can be implemented as long as the Gamma spectrum when the radioactive material is on the surface is known. In this paper, we will improve the performance when background spectrum is available; background contribution is normalized by using spectral comparison ratio (SCR), following by the MF operation. The resulting SCR MF approach outperforms the original MF approach and other widely used methods such as GC and EW.

APPROACH

Bin Projection

In practical field detection, it is necessary to calibrate all the data into the same energy range. Here, we sum the counts in an interval containing a few energy channels and divide it by the number of channels. Thus, we obtain a transformed spectrum. We call this process as bin projection (BP). Another advantage of BP is that it can transform a large number of sparse measurements in original channels into a few concrete measurements in several energy windows where random noise can be smoothed out.

Let an original L -channel energy spectrum be represented as $g(i)$ for $i = 1, 2, \dots, L$. The BP-transformed spectrum has K bins and the k -th bin includes n_k channels, i.e., $n_1 + n_2 + \dots + n_K = L$. The counts in the k -th bin $f(k)$ is calculated as

$$f(k) = \frac{1}{n_k} \sum_{i=n_1+\dots+n_{k-1}+1}^{i=n_1+\dots+n_k} g(i) \text{ for } k = 1, 2, \dots, K \quad (1)$$

All the following processes will be applied on the BP-transformed spectra. Fig. 1(a) illustrates the original target (i.e., buried radioactive waste) and background spectra, and Fig. 1(b) are those after BP where the bin width equals 354keV resulting in a 7-dimensional transformed spectra.

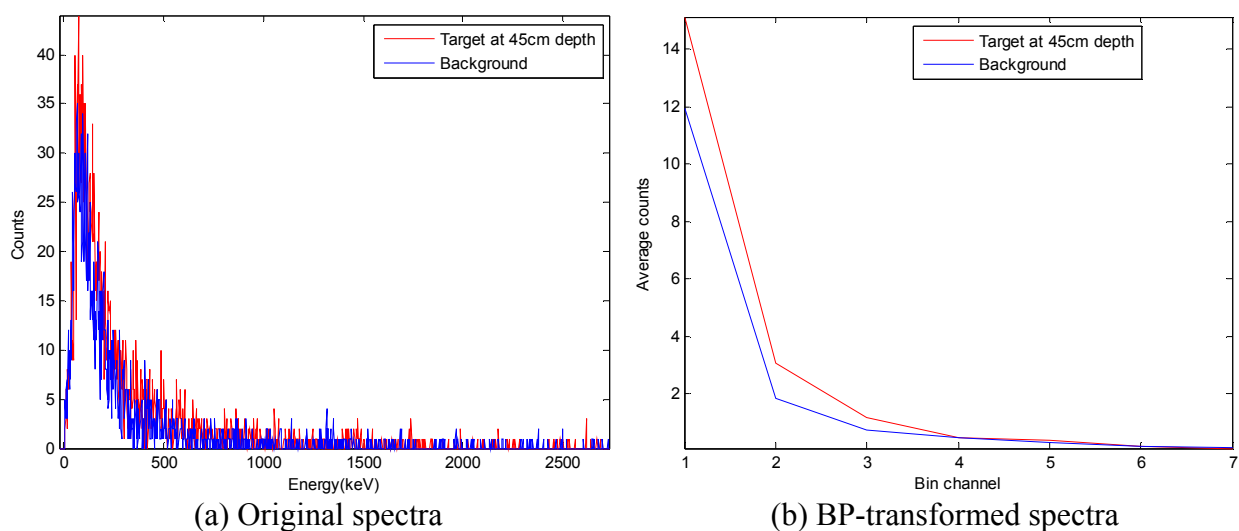


Figure 1: The energy spectra before and after BP.

Spectral Comparison Ratio (SCR)

The background brings about significant interference to buried target detection. To alleviate such interference, SCR is calculated for each measurement. It can magnify the difference between the current measurement and a reference measurement [2][3]. If the current measurement is similar with the reference, the SCR values will be close to zero. Thus, this process can reflect the actual discrepancy between the two measurements.

Here, a background measurement is chosen to be the reference. Then an SCR-transformed spectrum is equivalent to the one after background normalization. The SCR is computed as:

$$\mathbf{s}(n) = f(k) - \frac{f_B(k)}{f_B(n)} f(n) \quad \text{for } n \neq k \quad (2)$$

where k indicates the k -th bin which is used as the reference bin, and f_B denotes the background spectrum chosen as the reference measurement. Usually, the first bin ($k=1$) is the reference bin, then $\mathbf{s}(n)$ starts from $n = 2$ with $K-1$ samples. Fig. 2 shows the SCR results for the two spectra in Fig. 1(b). As we can see, these two spectra became more different than the original ones; in particular, the background measurement is close to 0.

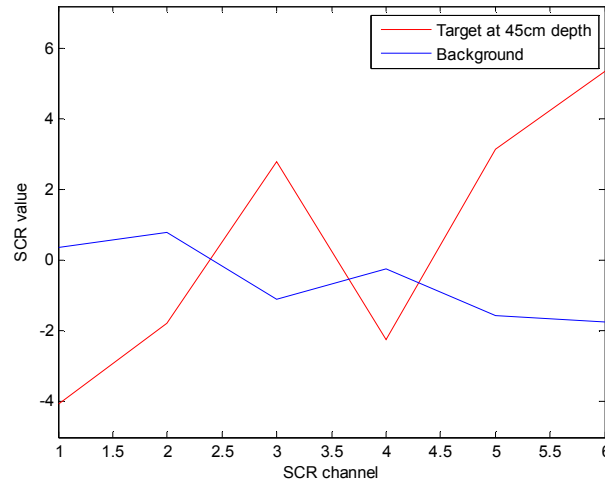


Figure 2: The spectra in Fig. 1(b) after applying SCR transformation.

Matched Filtering (MF)

The simplified MF operator can be expressed as:

$$\mathbf{y}(\mathbf{s}) = \frac{\mathbf{d}^T \boldsymbol{\Sigma}^{-1} \mathbf{s}}{\mathbf{d}^T \boldsymbol{\Sigma}^{-1} \mathbf{d}} \quad (3)$$

where \mathbf{s} is the input energy measurement vector after BP and SCR transforms, $\boldsymbol{\Sigma}^{-1}$ is the inverse of the background covariance matrix, \mathbf{d} is a column vector of the desired target energy spectral measurement. If the input \mathbf{s} includes the counts from radioactive material, i.e., target, the MF-output y should be a large value. By applying an appropriate threshold (determined with prior

information), the final decision for detection can be made.

When Σ is not full rank, the direct computation of its pseudoinverse matrix may not be accurate due to numerical errors. In this situation, we need to compute Σ^{-1} in another way which is shown as:

$$\Sigma^{-1} = \mathbf{V}\mathbf{\Lambda}^{-1}\mathbf{V}^T \quad (4)$$

where \mathbf{V} is the eigenvector matrix of Σ with each column being an eigenvector corresponding to a non-zero eigenvalue, and $\mathbf{\Lambda}$ is a diagonal matrix with each element being a non-zero eigenvalue in the same sequence in \mathbf{V} . Eq. (4) says that Σ^{-1} and Σ have the same set of eigenvectors, and their corresponding eigenvalues are inverse pairs.

We choose this MF method because it performs excellent in background suppression. Another reason is that this method requires the least amount of prior information. These advantages make the MF method more suitable for practical implementation.

Performance Evaluation

For a large dataset with many measurements, the nearest neighbor clustering method can be applied to the MF outputs. For a detection problem, which can be considered as two-class classification problem, the clustering can be conducted to form two clusters; for an m -class classification problem (e.g., to classify different SNM or classify the targets buried in different depths), then the clustering is to form c clusters. When training samples are available, they can be used to initiate the clustering algorithm. Then the detection/classification performance can be evaluated using overall accuracy p_a and Kappa coefficient k_a .

For quantitative performance evaluation, K-fold cross validation is adopted which is a commonly used statistical analysis method. It divides the original dataset into several sub-dataset. For each sub-dataset with k samples, one sample is randomly selected to be the validation sample to test the model, and the remaining $k-1$ samples are used as training data. Then one of the classification methods can be applied. The cross validation repeats k times as a sample in each dataset has the chance being selected once as a validation sample. A confusion matrix C can be obtained from these results, from which overall accuracy p_a and Kappa coefficient k_a can be derived.

The confusion matrix C for each method is computed, which is an $m \times m$ matrix for an m -class classification problem. Overall accuracy p_a and Kappa coefficient k_a are determined based on the confusion matrix, which are defined as $p_a = \frac{\sum_{i=1}^m c(i,i)}{\sum_{i=1}^m \sum_{j=1}^m c(i,j)}$ and $k_a = \frac{p_a - p_s}{1 - p_s}$, where

$$p_s = \sum_{i=1}^m \frac{\sum_{j=1}^m c(i,j) \sum_{j=1}^m c(j,i)}{(\sum_{i=1}^m \sum_{j=1}^m c(i,j))^2}$$

is the hypothetical probability of chance agreement. In addition, the confusion matrix C_d for detection is also computed, considering all the targets as one class and all the non-targets as the other. This two-class classification problem actually is a detection problem, and detection p_a and detection k_a can be determined accordingly. The performance of a method is claimed to be better if it yields greater values of p_a and k_a .

EXPERIMENT

In the experiment, we used a data consisting of 10 sub-datasets corresponding to a target buried at 7 different depths, nature ore with 2 different depths, and one background dataset. There were 24 samples in each sub-dataset, collected by a 10×10×40cm NaI detector. The target was a 105 mm penetrator with 4.3kg mass and was buried in soil at depths of 15cm, 23cm, 30cm, 45cm, 60cm, 75cm and 90cm. Nature ore was buried at depths of 45cm and 75cm. Sensor dwell time was varied from 0.1s, 0.25s, 0.5s, to 1s. All the measurements were normalized so that they were considered to be taken with 1s dwell time. The measured spectra consisted of 1024 channels with different energy ranges. The detailed information of this dataset is listed in Table I.

Table I. Attribute of a dataset with 10 different classes.

Sub-dataset	Attribute	Depth (cm)	Starting Energy (keV)	Ending Energy (keV)
1	target	15	-121	3256
2	target	23	-121	3256
3	target	30	-121	3256
4	target	45	-22	2730
5	target	60	-39	2713
6	target	75	-66	2612
7	target	90	-20	2865
8	Ore	45	-30	2693
9	Ore	75	-36	2707
10	Background	none	-8	2783

Four methods were implemented and compared: SCR MF, MF, GC, and EW method. In the SCR MF and MF methods, a spectrum when the target buried at 15cm was used as the desired target signature since the surface data was unavailable. In the EW method, two windows were determined, and the final output was the ratio of the sums in these two windows; the performance may be changed with the window selection, and the best result was presented here.

We chose the energy range from 0 to 2600 keV in the BP method and a bin length of 354 keV energy range was used. The BP-transformed data had 7 channels, and the SCR-transformed data had 6 channels. In the cross validation process, we chose $k=24$, i.e., that was 24-fold cross validation since there were 24 measurements in each sub-dataset.

Table II lists the ten-class confusion matrix for the SCR MF method with $p_a = 0.65$ and $k_a = 0.62$. Table III is the ten-class confusion matrix derived from Table II, where the first seven classes were grouped in a single class and the last three classes were for another class. The resulting detection $p_a = 0.83$ and detection $k_a = 0.69$. Tables IV and V show the performance for the MF method. Obviously, the off-diagonal elements were larger than those in Tables II and III, so both p_a and k_a were decreased. Tables VI and VII are for the GC method, and Tables VIII and IX are for the EW method. Table X summarizes the performance of the four methods. Due to the lack of surface measurement, the MF performance was degraded, which was similar to GC and EW methods. SCR MF could improve the MF performance with background normalization; in particular, SCR MF provided the best classification performance.

Table II. Confusion matrix of SCR MF (overall accuracy = 0.65, kappa coefficient = 0.62)

	15 cm	23 cm	30 cm	45 cm	60 cm	75 cm	90 cm	Ore45	Ore75	Bkg
15 cm	24	0	0	0	0	0	0	0	0	0
23 cm	0	24	0	0	0	0	0	0	0	0
30 cm	0	0	24	0	0	0	0	0	0	0
45 cm	0	0	0	24	0	0	0	0	0	0
60 cm	0	0	0	2	8	5	0	3	4	2
75 cm	0	0	0	1	2	7	1	2	6	5
90 cm	0	0	0	0	0	3	20	0	1	0
Ore45	0	0	0	1	4	3	0	5	2	9
Ore75	0	0	0	1	1	3	0	4	12	3
Bkg	0	0	0	1	3	1	0	6	4	9

Table III. Detection confusion matrix SCR MF (detection overall accuracy = 0.83; detection kappa coefficient = 0.60).

	target	non-target
target	145	23
non-target	18	54

Table IV. Overall confusion matrix for the MF method (overall accuracy = 0.54, kappa coefficient = 0.49).

	15 cm	23 cm	30 cm	45 cm	60 cm	75 cm	90 cm	Ore45	Ore75	Bkg
15 cm	24	0	0	0	0	0	0	0	0	0
23 cm	0	24	0	0	0	0	0	0	0	0
30 cm	0	0	24	0	0	0	0	0	0	0
45 cm	0	0	0	9	0	0	15	0	0	0
60 cm	0	0	0	0	17	1	0	2	1	3
75 cm	0	0	0	0	5	0	0	1	11	7
90 cm	0	0	0	6	0	0	18	0	0	0
Ore45	0	0	0	0	7	0	0	2	8	7
Ore75	0	0	0	0	3	5	0	3	8	5
Bkg	0	0	0	0	4	4	0	4	9	3

Table V. Detection confusion matrix for the MF method (detection overall accuracy = 0.80, detection kappa coefficient = 0.53).

	target	non-target
target	143	25
non-target	23	49

Table VI. Overall confusion matrix of the GC method (overall accuracy = 0.58, kappa coefficient = 0.54).

	15 cm	23 cm	30 cm	45 cm	60 cm	75 cm	90 cm	Ore45	Ore75	Bkg
15 cm	24	0	0	0	0	0	0	0	0	0
23 cm	0	24	0	0	0	0	0	0	0	0
30 cm	0	0	24	0	0	0	0	0	0	0
45 cm	0	0	0	23	0	0	1	0	0	0
60 cm	0	0	0	0	7	9	0	2	1	5
75 cm	0	0	0	0	10	0	0	6	2	6
90 cm	0	0	0	1	0	0	23	0	0	0
Ore45	0	0	0	0	3	3	0	4	5	9
Ore75	0	0	0	0	4	5	0	6	4	5
Bkg	0	0	0	0	2	2	0	7	5	8

Table VII. Detection confusion matrix of the GC method (detection overall accuracy = 0.83, detection kappa coefficient = 0.60).

	target	non-target
target	146	22
non-target	19	53

Table VIII. Overall confusion matrix of the EW method (overall accuracy = 0.57, kappa coefficient = 0.52).

	15 cm	23 cm	30 cm	45 cm	60 cm	75 cm	90 cm	Ore45	Ore75	Bkg
15 cm	21	3	0	0	0	0	0	0	0	0
23 cm	1	18	5	0	0	0	0	0	0	0
30 cm	0	2	19	3	0	0	0	0	0	0
45 cm	0	0	1	19	0	0	0	0	0	4
60 cm	0	0	0	1	10	2	0	4	2	5
75 cm	0	0	0	0	2	11	5	2	2	2
90 cm	0	0	0	0	3	4	17	0	0	0
Ore45	0	0	0	0	6	3	0	2	5	8
Ore75	0	0	0	0	6	1	0	4	8	5
Bkg	0	0	0	6	6	0	0	1	0	11

Table IX. Detection confusion matrix of the EW method (overall accuracy = 0.80, detection kappa coefficient = 0.50).

	target	non-target
target	147	21
non-target	28	44

Table X. Summary for the performance of the four algorithms.

	Overall accuracy	Kappa coefficient	Detection overall accuracy	Detection Kappa coefficient
SCR MF	0.65	0.62	0.83	0.60
MF	0.54	0.49	0.80	0.53
GC	0.58	0.54	0.83	0.60
EW	0.57	0.52	0.80	0.50

CONCLUSION

In this paper, we improve the MF method with SCR-based background normalization when background information is available. It can outperform other widely used techniques, such as GC and EW, even when the true desired target signature (i.e., surface measurement) is unavailable. In the future work, we will investigate the optimal bin width to be used in the BP process.

ACKNOWLEDGMENT

This research is supported by U.S. Army Engineer Research and Development Center at Vicksburg, Mississippi.

REFERENCES

1. Q. DU, N. H. YOUNAN, C. WAGGONER, AND D. RODERS, "Effective detection of buried radioactive waste," Proceedings of Waste Management Conference (2009).
2. D. M. PFUND, R. C. RUNKLE, K. K. ANDERSON, AND K. D. JARMAN, "Examination of count-starved gamma spectra using the method of spectral comparison ratios," IEEE Transactions on Nuclear Science, 54 (4): 1232-1238 (2007).
3. K. K. ANDERSON, K. D. JARMAN, M. L. MANN, D. M. PFUND, AND R. C. RUNKLE, "Discriminating nuclear threats from benign sources in gamma-ray spectra using a spectral comparison ratio method," Journal of Radioanalytical and Nuclear Chemistry, 276 (3): 713-718 (2008).
4. R. O. DUDA, P. E. HART, AND D. G. STORK, Pattern Classification, 2nd ed., Canada: John Wiley & Sons, Inc., 402-582 (2001).
5. E. R. SICILIANO, J. H. ELY, R. T. KOUZES, B. D. MILBRATH, J. E. SCHWEPPE, D. C. STROMSWOLD, "Comparison of PVT and NaI(Tl) scintillators for vehicle portal monitor applications," Nuclear Instruments and Methods in Physics Research A, 550: 647-674 (2005).
6. R. T. KOUZES, J. H. ELY, B. D. MILBRATH, J. E. SCHWEPPE, E. R. SICILIANO, D. C. STROMSWOLD, "Spectroscopic and non-spectroscopic radiation portal applications to border security," IEEE Nuclear Science Symposium Conference Record, 321-325 (2005).
7. R. T. KOUZES AND J. H. ELY, "The role of spectroscopy versus detection for border security," Journal of Radioanalytical and Nuclear Chemistry, 276 (3): 719-723 (2008).

8. D. C. STROMSWOLD, E. R. SICILIANO, J. E. SCHWEPPE, J. H. ELY, B. D. MILBRATH, R. T. KOUZES, AND B. D. GEELHOOD, "Comparison of plastic and NaI(Tl) scintillators for vehicle portal monitor applications," Nuclear Instruments and Methods in Physics Research Section A: Accelerators, Spectrometers, Detectors and Associated Equipment, 550 (3): 647-674 (2005).
9. J. H. ELY, R. T. KOUZES, B. D. GEELHOOD, J. E. SCHWEPPE, AND R. A. WARNER, "Discrimination of naturally occurring radioactive material in plastic scintillator material," IEEE Transactions on Nuclear Science, 51 (4): 1672-1676 (2004).
10. J. H. ELY, R. T. KOUZES, J. E. SCHWEPPE, E. R. SICILIANO, D. M. STRACHAN, AND D. R. WEIER, "The use of energy windowing to discriminate SNM from NORM in radiation portal monitors," Nuclear Instruments and Methods in Physics Research, 560 (2): 373-387 (2006).
11. S. P. LIU, J. GONG, F. H. HAO, G. C. HU, "Template identification technology of nuclear warheads and components," Chinese Physics B, 17 (2): 363-369 (2008).